available at www.sciencedirect.com
journal homepage: www.europeanurology.com

European Association of Urology

Platinum Priority – Prostate Cancer

Editorial by John R. Prensner and Felix Y. Feng on pp. 327–328 of this issue

The Long Noncoding RNA TTTY15, Which Is Located on the Y Chromosome, Promotes Prostate Cancer Progression by Sponging let-7

Guang'an Xiao [a,b,†], *Jingjing Yao* [a,b,†], *Depei Kong* [a,b,†], *Chen Ye* [a,b], *Rui Chen* [a,b], *Li Li* [c], *Tao Zeng* [c], *Liujun Wang* [c], *Wei Zhang* [a,b], *Xiaolei Shi* [a,b], *Tie Zhou* [a,b], *Jing Li* [a,b], *Yue Wang* [b,c], *Chuan Liang Xu* [a,b], *Junfeng Jiang* [a,b,c,**], *Yinghao Sun* [a,b,*]

[a] *Department of Urology, Shanghai Changhai Hospital, Second Military Medical University, Shanghai, China;* [b] *Shanghai Key Laboratory of Cell Engineering, Second Military Medical University, Shanghai, China;* [c] *Department of Histology and Embryology, College of Basic Medicine, Second Military Medical University, Shanghai, China*

Article info

Article history:
Accepted November 6, 2018

Associate Editor:
James Catto

Statistical Editor:
Andrew Vickers

Keywords:
CRISPR/Cas9
Long noncoding RNAs
Prostate cancer
TTTY15
Y chromosome

Abstract

Background: The link between prostate cancer (PCa) development and aberrant expression of genes located on the Y chromosome remains unclear.
Objective: To identify Y-chromosomal long noncoding RNAs (lncRNAs) with critical roles in PCa and to clarify the corresponding mechanisms.
Design, setting, and participants: Aberrantly expressed lncRNAs on the Y chromosome were identified using transcriptome analysis of PCa clinical samples and cell lines. Biological functions and molecular mechanisms of the lncRNAs were revealed using in vitro and in vivo experimental methods.
Outcome measurements and statistical analysis: Experiments and outcome measurements were performed in duplicate or triplicate. Wilcoxon signed-rank test was employed for comparison of RNA levels in clinical cohorts. Analysis of variance was employed for comparisons among multiple groups.
Results and limitations: In most patients with PCa, TTTY15 was the most elevated lncRNA located on the Y chromosome. Knockout of this lncRNA by two different CRISPR-Cas9 strategies suppressed PCa cell growth both in vitro and in vivo. TTTY15 promoted PCa by sponging the microRNA let-7, consequently increasing CDK6 and FN1 expression. FOXA1 is an upstream regulatory factor of TTTY15 transcription.
Conclusions: The Y-chromosomal lncRNA TTTY15 was upregulated in most PCa tissues and could promote PCa progression by sponging let-7.
Patient summary: We found that TTTY15 levels were frequently elevated in prostate cancer (PCa) tissues compared with those in paracancerous normal tissues in a large group of PCa patients, and we observed a tumour suppressive effect after TTTY15 knockout using CRISPR/Cas9. These results may have therapeutic implications for PCa patients.

* Corresponding author. Department of Urology, Shanghai Changhai Hospital, Second Military Medical University, Shanghai 200433, China. Tel.: +86 13601 607755; Fax: +86 21 3505 0006.
E-mail addresses: jeffrey99@qq.com (J. Jiang), sunyhsmmu@126.com (Y. Sun).
** Corresponding author. Department of Urology, Shanghai Changhai Hospital, Second Military Medical University, Shanghai 200433, China. Tel.: +86 13671562412.
E-mail address: jeffrey99@qq.com (J. Jiang).
† These authors contributed equally to this work.

https://doi.org/10.1016/j.eururo.2018.11.012
0302-2838/

1. Introduction

Prostate cancer (PCa) is one of the most common malignant tumours worldwide [1–4]. With the progress in research technology, an increasing number of genetic factors have been shown to be involved in the generation and progression of PCa [5–11]. However, the role of Y-chromosome–located factors in PCa development remains largely unknown.

As the only male-determining chromosome, the Y chromosome plays important roles in the development of male-specific organs and may be involved in many male-specific diseases, such as PCa. Y-chromosome-located factors may be potential gene therapy targets with unique advantage for the future treatment of PCa, because Y chromosome is haploid and has much higher efficiency for genome-editing strategy than other chromosomes. The loss of Y-chromosomal factors may have limited side effects on the whole body because women survive healthily without these factors. Identification of Y-chromosomal factors with critical roles in PCa may not only improve our understanding of PCa development, but also further enable diagnosis or treatment of this disease [12–15]. However, the overall function of the Y chromosome as well as that of its resident genes in PCa remains controversial [16,17].

In recent years, lncRNAs have been shown to play important roles in many physiological and pathological conditions, including PCa [18,19]. Although some lncRNAs have been reported to participate in PCa generation and progression, such as SChLAP1 [20], HOTAIR [21], PCA3 [22], PCAT1 [23], NEAT1 [24], and CTBP1-AS [25], lncRNAs located on the Y chromosome have not been systematically studied in PCa.

In the current study, we found that the Y-chromosomal lncRNA TTTY15 was upregulated in most PCa tissues and could promote PCa progression by sponging let-7. We also identified FOXA1 as an upstream transcription factor (TF) of TTTY15.

2. Patients and methods

2.1. Patients and specimens

All specimens were obtained and handled using standard protocols in Changhai Hospital after obtaining informed consent from the patients. The pairs of matched tumour and normal tissues were used for transcriptome analysis and quantitative reverse transcription polymerase chain reaction (qRT-PCR) validation. A tissue microarray (TMA) was constructed using archived pathological formalin-fixed, paraffin-embedded specimens.

2.2. Construction of the TTTY15 knockout cell model

Two strategies for TTTY15 knockout (KO) mediated by the CRISPR/Cas9 system were designed. The first was a CRISPR/Cas9-based TTTY15 cut-off strategy, which is shown in Fig. 1A. The second involved the insertion of a terminator sequence mediated by CRISPR/Cas9, as shown in Fig. 2A.

2.3. Animal studies

Briefly, 3×10^6 PCa cells subjected to various treatments were subcutaneously injected into 4-wk-old male nude mice. All procedures adhered to the guidelines of the Animal Care and Use Committee of the Second Military Medical University, Shanghai, China.

2.4. Statistics

Statistical analyses were conducted using SPSS version 21.0 software, and graphs were generated using GraphPad Prism 6.0 software.

2.5. Detailed experimental methods and materials

Detailed descriptions of the experimental procedures and statistical analyses are presented in Supplementary material.

3. Results

3.1. Expression of the Y chromosome–transcribed lncRNA TTTY15 is frequently elevated in PCa

We previously established a transcriptome database using 65 pairs of tumour and normal tissues from Chinese PCa patients [26], and thus, here, we employed this database to first analyse all the lncRNAs located on the Y chromosome based on the fold changes and found that TTTY15 showed the greatest expression increase in PCa tissues compared with paired control tissues (Fig. 3A). In addition, TTTY15 levels were frequently elevated in PCa tissues compared with those in paracancerous normal tissues (Fig. 3B), which was further validated in additional 35 pairs of PCa tumour and normal tissues by qRT-PCR (Fig. 3C). In addition, the change in TTTY5 expression in PCa was not limited to Chinese patients; increased TTTY15 expression was also observed in PCa tissues from patients of other ethnicities in The Cancer Genome Atlas (TCGA; $n = 52$; Fig. 3D). Furthermore, we performed transcriptome sequencing using an additional larger clinical sample cohort comprising 145 pairs of PCa tumour and normal samples and observed increased TTTY15 expression in PCa (Fig. 3E). TTTY15 RNA in situ hybridisation results from our TMA cohort with 70 tumour samples and 16 normal samples confirmed the same phenomenon (Fig. 3F).

3.2. TTTY15 promotes PCa cell proliferation and migration

Next, we analysed the potential roles of TTTY15 in PCa in vitro. Based on publicly available data, we found relatively high levels of TTTY15 in the prostate compared with those in most other human tissues (Supplementary Fig. 1). Basal TTTY15 expression was higher in the tested PCa cell lines than in the normal prostate cell line RWPE1 (Fig. 4A). After screening seven siRNAs, we found that si-14 and si-2366 efficiently knocked down TTTY15 expression in PCa cells (Supplementary Figs. 2A, 2B, and 3A). TTTY15 knockdown (KD) did not have a substantial effect on cell apoptosis (Supplementary Fig. 2C) but significantly decreased the proliferation of the PCa cell line DU145, according to CCK-8

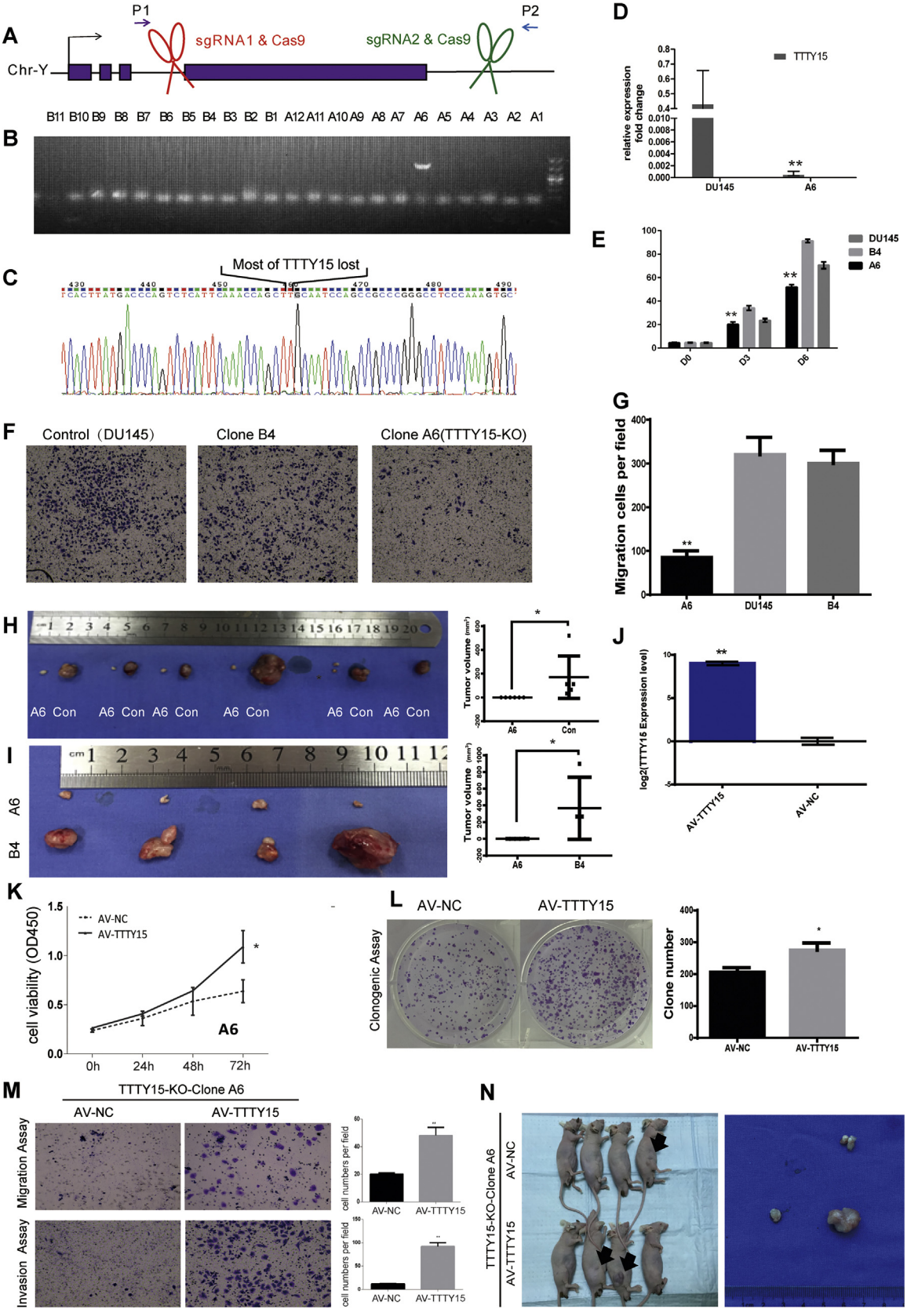

Fig. 1 – TTTY15 knockout using CRISPR-Cas9 shows that TTTY15 promotes prostate cell proliferation, migration, and invasion. (A) A strategy for TTTY15 knockout using CRISPR-Cas9–mediated double cleavage. (B) PCR results for 30 single-cell clones using primers P1 and P2, and the results are shown for clone A6 that carries the TTTY15 resection genotype. (C) Sequencing results of the PCR product revealed deletion of the majority of the TTTY15 sequence. (D) Relative expression of TTTY15 in clone A6, determined by qRT-PCR. Beta-actin was used as the reference. The data are presented as the mean ± SD. *$p < 0.05$ and **$p < 0.01$, Student t test ($n = 3$). (E) Cell proliferation was assessed in TTTY15 knockdown DU145 cells using a CCK-8 kit.

(Fig. 4B) and EdU (Fig. 4C and Supplementary Fig. 2D) assays, and similar results were observed in the LNCaP cell line (Supplementary Fig. 3B and 3C). Additionally, si-14 and si-2366 significantly inhibited the ability of DU145 cells to form colonies (Fig. 4D). Furthermore, the migration and invasion of DU145 (Fig. 4E) and LNCaP (Supplementary Fig. 3D) cells were reduced after TTTY15 KD. In contrast, TTTY15 overexpression induced by adenovirus infection increased the ability of PCa cells, such as DU145 (Fig. 4F and Supplementary Fig. 2E and 2F) and PC3 (Supplementary Fig. 4A) cells, to form colonies and increased the proliferation of PCa cell lines, including DU145 (Fig. 4G and 4H), LNCaP (Supplementary Fig. 3E and 3F), and PC3 (Supplementary Fig. 4B) cell lines. TTTY15 overexpression also increased the migration and invasion of DU145 (Fig. 4I), LNCaP (Supplementary Fig. 3G), and PC3 (Supplementary Fig. 4C) cells. Thus, TTTY15 promoted the proliferation and migration of both an androgen receptor (AR)-positive PCa cell line (LNCaP) and AR-negative cell lines (DU145 and PC3), and we found that TTTY15 was not androgen responsive (Fig. 4J and Supplementary Fig. 3H).

3.3. CRISPR-mediated TTTY15 deletion suppresses the tumour phenotypes of PCa cells

To further investigate the function of TTTY15 in PCa cells, we employed a KO strategy that is considered reliable for genotype-phenotype study. We designed a CRISPR strategy to cleave two sites (Supplementary Fig. 5A–C) and resect the majority of the TTTY15 sequence (Fig. 1A). We obtained one positive cell clone, A6, which exhibited the TTTY15 resection genotype and decreased TTTY15 RNA expression levels (Fig. 1B–D) from 30 single-cell clones selected after transfection, and utilised a TTTY15-unresected cell clone (B4) as the negative control.

We further found that the proliferation of A6 cells was decreased compared with that of the parental DU145 and B4 cells (Fig. 1E and Supplementary Fig. 5D and 5E). Interestingly, A6 cells also showed more scattered growth (Supplementary Fig. 5F) and reduced migration and invasion compared with DU145 or B4 cells (Fig. 1F and 1G and Supplementary Fig. 5G and 5H). Additionally, in line with the KD experiment (Supplementary Fig. 2C), KO of TTTY15 also exerted a relatively mild effect on cell apoptosis following H_2O_2 treatment (Supplementary Fig. 6A), but a higher number of apoptotic cells was observed in the docetaxel setting (Supplementary Fig. 6B). More interestingly, the results of several animal studies showed that the growth of tumours derived from A6 cells was substantially reduced compared with that of tumours derived from control cells (Fig. 1H and 1I, and Supplementary Fig. 6C). Moreover, identification of A6 cells was authenticated by short tandem repeat profiling, and they showed maximum similarity with DU145 cells (Supplementary Fig. 6D). In rescue experiments, we found that cell growth (Fig. 1J–L), migration, and invasion (Fig. 1M) were all significantly restored after overexpression of TTTY15 via adenovirus infection compared with the controls. Furthermore, in vivo experiments showed increased growth of tumours derived from TTTY15-overexpressing A6 cells (Fig. 1N).

3.4. Use of a novel CRISPR strategy for lncRNA KO indicates a role for TTTY15 in promoting PCa

To exclude unexpected effects of TTTY15 KO employing the large segment deletion strategy, we further invented a novel CRISPR strategy for lncRNA KO by knocking a “transcription terminator” sequence into the site immediately following the transcription start site through a nonhomologous end-joining mechanism (Fig. 2A). We successfully obtained four TTTY15-KO cell clones from 10 selected single-cell clones, as determined by genome PCR and Sanger sequencing (Fig. 2B–D) as well as RT-PCR analysis (Fig. 2E). Based on these data, we confirmed that TTTY15 was knocked out through this strategy.

Then, we explored the phenotypic differences between these TTTY15 KO clones (TKO2 and TKO8) and control DU145 cells. Consistent with the A6 cell results, TKO2 and TKO8 cells also exhibited reduced cell growth (Fig. 2F), migration, and invasion (Fig. 2G and Supplementary Fig. 7F). Additionally, xenografts in mice derived from TKO2 and TKO8 cells showed substantially reduced growth compared with that of the control cells (Fig. 2H). Similarly, overexpression of TTTY15 in TKO2 and TKO8 cells increased cell proliferation (Fig. 2I and 2J, and Supplementary Fig. 7A, 7D, and 7E), migration, and invasion (Fig. 2K and 2L, and Supplementary Fig. 7B, 7C, 7G, and 7H).

3.5. TTTY15 promotes PCa progression by sponging let-7 and upregulating CDK6 and FN1

To explore the mechanism underlying the cancer-promoting effect of TTTY15, we first determined via RNAscope hybridisation and nuclear plasma separation that TTTY15 was located mainly in the cytoplasm (Fig. 5A and B). Then, we explored whether TTTY15 functions as a competing endogenous RNA (ceRNA) in PCa cells, as reported in our previous study [27,28]. Using miRDB [29] and miRanda software [30], 12 microRNAs (miRNAs) were predicted as candidate targets of TTTY15 (Supplementary Fig. 8A and 8B)

$^{*}p < 0.05$ and $^{**}p < 0.01$, repeated measures ANOVA ($n = 3$). (F) Transwell migration assay using TTTY15 knockout DU145 cells. Clone A6 is the TTTY15 knockout DU145 single-cell clone; B4 is the DU145 single-cell clone in which TTTY15 knockout failed. (G) Statistical analysis of the results is shown in (F). $^{**}p < 0.01$, *t* test ($n = 3$). (H and I) Xenograft experiments showed reduced growth of clone A6 in nude mice. (J) TTTY15 was significantly increased after infection with TTTY15 adenovirus. (K) Cell proliferation was assessed after TTTY15 overexpression in Clone A6 using a CCK-8 kit. $^{*}p < 0.05$ and $^{**}p < 0.01$, repeated measures ANOVA ($n = 3$). (L) Clonogenic assay after TTTY15 overexpression in clone A6 ($n = 3$). (M) Transwell migration and invasion assays after TTTY15 overexpression in clone A6. $^{*}p < 0.05$ and $^{**}p < 0.01$, ANOVA ($n = 3$). (N) Xenograft experiments showed restoration of the growth of clone A6 after TTTY15 overexpression in nude mice. ANOVA = analysis of variance; PCR = polymerase chain reaction; qRT-PCR = quantitative reverse transcription polymerase chain reaction; SD = standard deviation. (Note to readers: Figure 1F was updated post-acceptance).

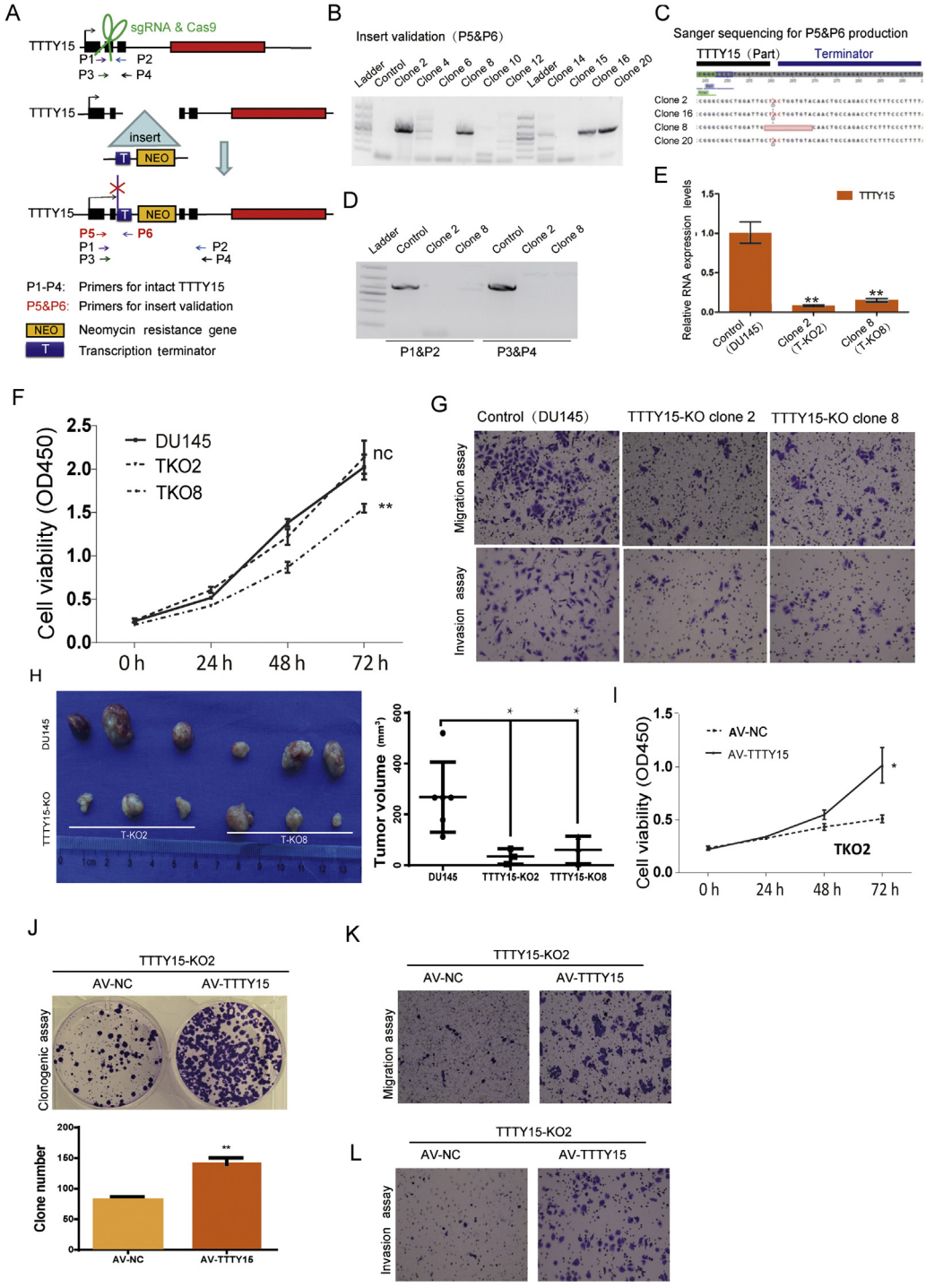

Fig. 2 – The TTTY15 KO cell model constructed using a novel "knock-in" to "knockout" strategy mediated by CRISPR/Cas9 shows reduced proliferation, migration, and invasion. (A) The strategy used to construct the TTTY15 KO cell model. A specific sequence containing a transcription termination signal, the neomycin resistance gene, and an EGFP expression cassette was knocked into the TTTY15 coding region. (B) Insert validation using gel electrophoresis after PCR. The primers (P5 and P6) primed the amplification of products spanning the TTTY15 and insert sequences. (C) PCR products from clones 2, 16, 8, and 20 were sequenced, and the insert sequence was detected with two different variants. (D) The primers (P1 and P2, P3 and P4) primed the efficient amplification of products from the TTTY15 coding sequence if no insert knock-in genomic DNA was present. (E). Expression of TTTY15 was quantified by qRT-PCR. $^{*}p < 0.05$ and $^{**}p < 0.01$, ANOVA ($n = 3$) (F) Proliferation of TKO2 and TKO8 cells was assayed using a CCK-8 kit. $^{*}p < 0.05$ and $^{**}p < 0.01$, repeated measures ANOVA ($n = 3$). (G) Migration and invasion of TKO2 and TKO8 cells was determined using Transwell assays. $^{*}p < 0.05$ and $^{**}p < 0.01$, ANOVA ($n = 3$). (H) Xenografts of a novel TTTT15 KO cell model showed reduced growth. (I) Cell proliferation was assessed using a CCK-8 kit after the rescue of TTTY15 expression. $^{*}p < 0.05$ and $^{**}p < 0.01$, repeated measures ANOVA ($n = 3$). (J) TKO2 cell proliferation was evaluated using a clonogenic assay after TTTY15 rescue. (K and L) Migration and invasion were examined using Transwell assays after TTTY15 rescue. Representative images are shown. ANOVA = analysis of variance; KO = knockout; PCR = polymerase chain reaction; qRT-PCR = quantitative reverse transcription polymerase chain reaction.

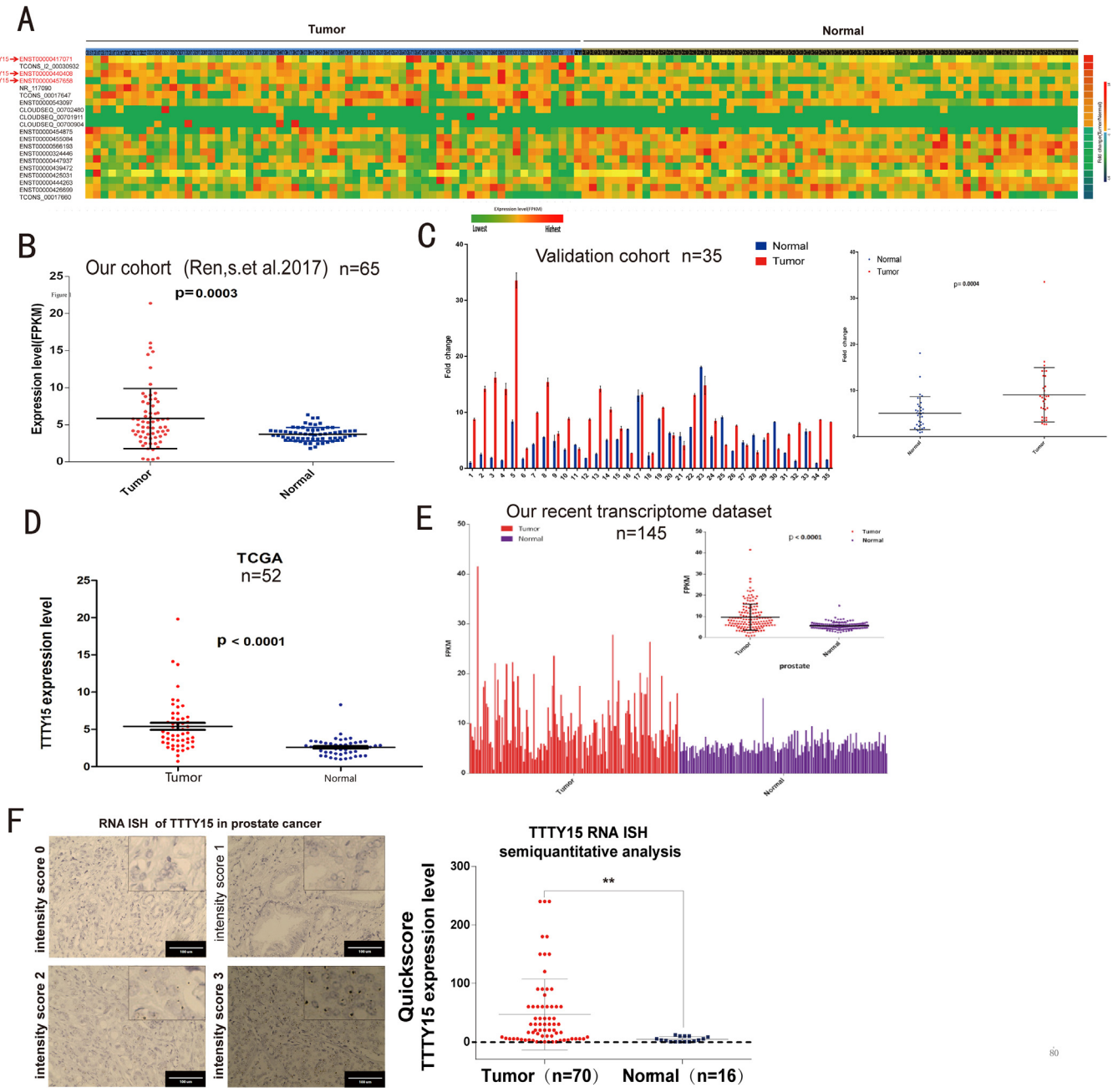

Fig. 3 – Expression of the lncRNA TTTY15 is frequently elevated in prostate cancer (PCa). (A) RNA expression in 65 pairs of paired PCa tissues and adjacent normal prostate tissues was quantified by RNA sequencing. The heat map shows the expression levels in each tumour and paired normal tissue (left panel) [26], and fold changes were normalised to the levels in normal tissues (right panel). (B) Quantitative statistical analysis of TTTY15 levels in 65 paired samples. (C) Relative expression of TTTY15 was determined in 35 pairs of PCa and adjacent normal tissues by qRT-PCR and normalised to beta-actin expression. (D) TTTY15 expression level (TCGA data; $n = 52$, data were downloaded in June 2017). (E) Statistical analysis of TTTY15 levels in an additional larger clinical sample cohort comprising 145 pairs of PCa tumour and normal samples quantified by RNA sequencing. (F) The left panel shows the representative images of TTTY115 staining after probes were hybridised to the tissue sections. The semiquantitative analysis results are shown in the right panel. ISH = in situ hybridisation; lncRNA = long noncoding RNA; qRT-PCR = quantitative reverse transcription polymerase chain reaction; TCGA = The Cancer Genome Atlas. $^{*}p < 0.05$ and $^{**}p < 0.01$, Wilcoxon signed-rank test.

and were then confirmed with a dual luciferase reporter assay (Fig. 5C). In addition, inhibition of TTTY15 expression by these miRNA mimics in DU145 cells suggested that these miRNAs were "sponged" by TTTY15 (Fig. 5D).

Next, we assessed the ceRNA hypothesis through quantitative measurement of TTTY15 and miRNA abundance in PCa cells and tissues. The levels of TTTY15 in the PCa cell lines DU145, C42-B, and LNCaP varied from 29 to 136 copies per cell, and the levels in the normal prostate cell line RWPE1 and the TTTY15 KO cell line A6 was nearly 0 copies per cell (Fig. 5E). Based on TCGA BCGSC miRNA profiling data ($n = 551$) and our absolute quantification

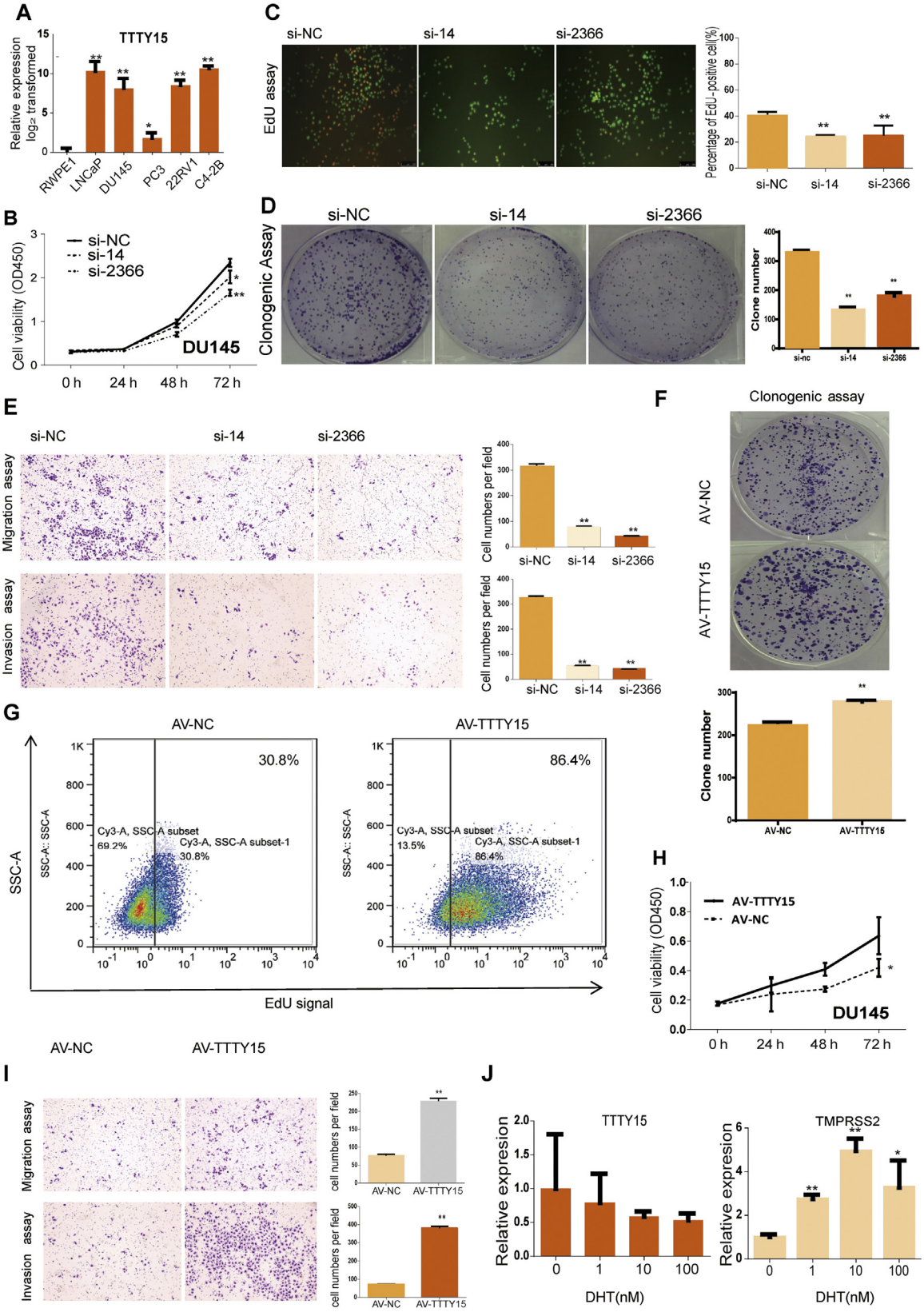

Fig. 4 – Effects of TTTY15 on PCa phenotypes in vitro. (A) Basal expression levels of TTTY15 in PCa cell lines (DU145, LNCaP, PC3, 22RV1, and C42B) and a normal prostate cell line (RWPE1) were determined using qRT-PCR. Beta-actin was used as the reference. The data are presented as the mean ± SD. $^{*}p < 0.05$ and $^{**}p < 0.01$, ANOVA ($n = 3$). (B) Cell proliferation was assessed after TTTY15 knockdown in DU145 cells using a CCK-8 kit. $^{*}p < 0.05$ and $^{**}p < 0.01$, repeated measures ANOVA ($n = 3$). (C) EdU cell proliferation assay results in DU145 cells after TTTY15 knockdown. Statistical analysis of the results is shown in addition to the data. $^{*}p < 0.05$ and $^{**}p < 0.01$, chi-square analysis ($n = 3$). (D) Clonogenic assay in TTTY15 knockdown DU145 cells. The quantitative data are shown beside the images. $^{*}p < 0.05$ and $^{**}p < 0.01$, ANOVA ($n = 3$). (E) Transwell migration and invasion assay results using TTTY15 knockdown DU145 cells. The quantitative data are shown beside the images. $^{*}p < 0.05$ and $^{**}p < 0.01$, ANOVA ($n = 3$). (F) Clonogenic assay in

assays for representative miRNAs, we finally found that let-7a, let-7b, let-7c, and let-7f among the candidate miRNAs were expressed at levels similar to those of TTTY15 in PCa tissues and cells, while other miRNAs, such as let-7d, were expressed at much lower levels and therefore may not to be affected by the TTTY15 "sponge" activity (Fig. 5F and 5G, and Supplementary Fig. 8C). Thus, the let-7 family members let-7a, let-7b, let-7c, and let-7f represent the key miRNAs in this ceRNA network.

We then tested the expression levels of 22 reported let-7 targets, and found that most were decreased after TTTY15 KO (Fig. 5H) and increased after TTTY15 overexpression in A6 cells (Fig. 5I). Among these targets, CDK6 and FN1 were selected for further validation, and they showed decreased expression in TKO2 and TKO8 cells as well (Fig. 5J). Moreover, transfection with let-7 mimics significantly downregulated CDK6 and FN1 expression (Fig. 5K). At the protein level, CDK6 and FN1 levels were decreased after TTTY15 KD (Fig. 5L) and KO (Fig. 5M). Additionally, overexpression of a TTTY15-Mut plasmid encoding mutated let-7 binding site had little effect on CDK6 and FN1 expression (Fig. 5N and Supplementary Fig. 8B). Gene set enrichment analysis showed that genes affected by let-7 miRNA family was negatively enriched with TTTY15 KO (Fig. 5O). These data supported the hypothesis that TTTY15 could promote PCa progression by sponging let-7.

3.6. *FOXA1 is an upstream regulatory TF of TTTY15 in PCa cells*

We first confirmed that the DNase I hypersensitive sites and epigenetic markers of active transcription were enriched in the promoter region of TTTY15 (Supplementary Fig. 9A). As TTTY15 was unrelated to AR, as mentioned above, we explored whether other TFs were involved in TTTY15 regulation. We examined the expression levels of previously reported PCa-related TFs in TCGA and our cohort (Supplementary Fig. 9B and 9C) and found that only FOXA1 and HOXB13 were positively correlated with TTTY15 expression (Fig. 6A and Supplementary Fig. 9E and 9F). Given that only downregulated FOXA1 could decrease TTTY15 (Fig. 6B) and its expression levels were significantly increased in PCa tissues (Fig. 6C and 6D), we focused on FOXA1 for further study. We then predicted the potential FOXA1 binding sites in the promoter of TTTY15 (Fig. 6E and Supplementary Fig. 9D) and confirmed their direct binding using ChIP experiments (Fig. 6F). Moreover, FOXA1 overexpression increased TTTY15 expression in DU145 cells (Fig. 6G). Thus, for the first time, we have revealed the function and mechanism of TTTY15 in PCa, which is shown in Fig. 6H.

4. Discussion

The Y chromosome has been reported to play a role in PCa carcinogenesis [31–34]. Different Y lineages may partially contribute to the differences in PCa incidence between American and Asian populations [31]. However, some researchers have reported evidence against this role of the Y chromosome in PCa in European populations [15,35]. Recently, in a study of three large prospective cohorts, mosaic loss of the Y chromosome (mLOY) showed a significant association with PCa risk (odds ratio = 1.35, $p = 0.024$) [36]. Therefore, the function of the Y chromosome in PCa remains controversial. Our study showed that the Y chromosome–transcribed lncRNA TTTY15 may participate in PCa development. The vague mLOY may cause mutation or exchange of TTTY15, which may partially explain certain observations, indicating that the Y chromosome may participate in PCa.

CRISPR-Cas9 is a specific and accurate genome editing tool for basic research, and shows a bright future for clinical applications [37]. However, due to the relatively low efficiency of obtaining an lncRNA KO homozygote, very few lncRNAs have been researched using KO lines, particularly in PCa. Here, we used two CRISPR strategies for KO TTTY15, and these CRISPR-based results may substantially improve the reliability of findings showing that TTTY15 plays roles in PCa. Based on these results, we believe that TTTY15 represents a potentially good CRISPR target for future PCa treatments. However, our experiments also have limitations. One problem is the heterogeneity of PCa cells. Although three TTTY15 KO clones derived from two KO methods were selected for the function and mechanism studies, the influence of cell heterogeneity cannot be completely excluded. Additional studies are warranted.

In the current study, we explored the upstream and downstream mechanisms of TTTY15 in PCa. FOXA1 plays an important role in PCa development, and it can function in an AR-dependent [7,38] or AR-independent [7,39,40] fashion. Here, we also showed that TTTY15 regulated by FOXA1 had roles in both AR-positive and AR-negative PCa cells, which enhances our understanding of the downstream mechanism of FOXA1 in PCa. In addition, we assessed the hypothesis that TTTY15 functions as a ceRNA and "sponges" members of the let-7 family to upregulate FN1 and CDK6 expression in PCa cells. FN1 plays a key role in cancer metastasis [41,42], and CDK6 regulates cell proliferation [43]. Therefore, we suggest that TTTY15 connects these factors into a FOXA1–TTTY15–let-7–FN1/CDK6 network. Further systematic studies are needed to elucidate the regulatory mechanisms more comprehensively.

TTTY15-overexpressing DU145 cells. The quantitative data are shown under the images. $^{*}p < 0.05$ and $^{**}p < 0.01$, *t* test ($n = 3$). (G) EdU cell proliferation assay results measured by flow cytometry in TTTY15-overexpressing DU145 cells. (H) Proliferation of TTTY15-overexpressing DU145 cells, determined using a CCK-8 kit. $^{*}p < 0.05$ and $^{**}p < 0.01$, repeated measures ANOVA ($n = 3$). (I) Transwell migration and invasion assays using TTTY15-overexpressing DU145 cells. Statistical analysis of the results is shown in addition to the images. $^{**}p < 0.01$, Student *t* test ($n = 3$). (J) An androgen-sensitivity assay using LNCaP cells showed that androgen did not alter TTTY15 expression significantly. TMPRSS2 cells were used as the positive control. RNA levels were examined by qRT-PCR. Beta-actin was used as the reference. The data are presented as the mean ± SD. $^{*}p < 0.05$ and $^{**}p < 0.01$, ANOVA ($n = 3$). ANOVA = analysis of variance; PCa = prostate cancer; qRT-PCR = quantitative reverse transcription polymerase chain reaction; SD = standard deviation.

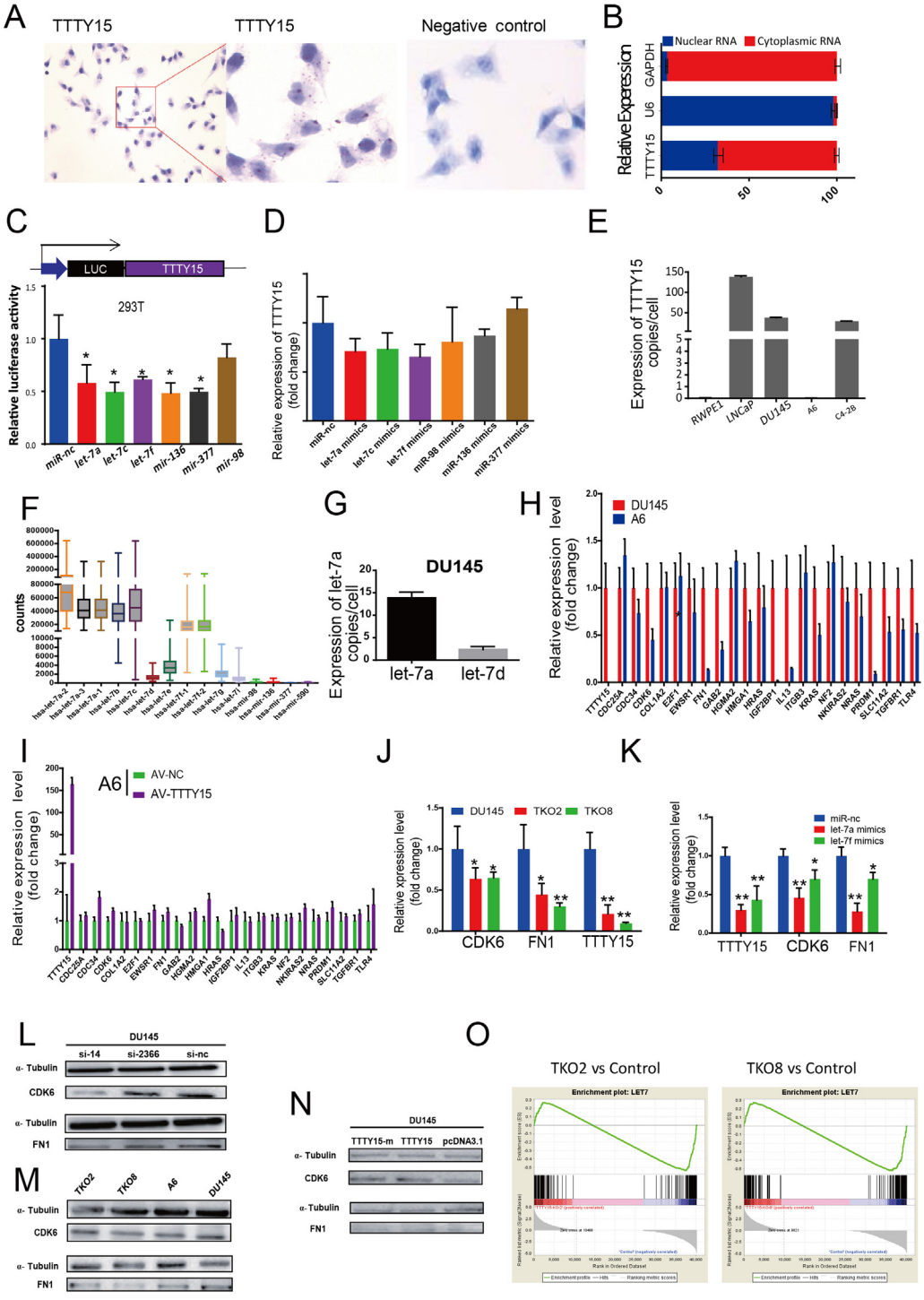

Fig. 5 – TTTY15 functions as an RNA sponge by binding to let-7 family members to regulate CDK6 and FN1 expression. (A) RNA ISH in DU145 cells showed that TTTY15 was mainly located in the cytoplasm. (B) Analyses of nuclear and cytoplasmic extracts revealed that approximately two-thirds of TTTY15 were located in the cytoplasm. The data are presented as the mean ± SD. (C) A dual luciferase reporter assay was performed to test the binding. $^{*}p < 0.05$ and $^{**}p < 0.01$, ANOVA ($n = 3$). (D) TTTY15 expression was downregulated after transfection with representative microRNAs. $^{*}p < 0.05$ and $^{**}p < 0.01$, ANOVA ($n = 3$). (E) Absolute quantification of TTTY15 expression. The data are presented as the mean ± SD ($n = 3$). (F) Target microRNA expression in PCa and normal tissues from TCGA dataset ($n = 551$); let-7a, let-7b, let-7c, and let-7f were expressed at higher levels than other miRNAs. (G) Absolute quantification of let-7a and let-7d levels. The data are presented as the mean ± SD ($n = 3$). (H and I) Expression of genes targeted by the let-7 family in the TTTY15 KO model and rescue models. $^{*}p < 0.05$ and $^{**}p < 0.01$, Student t test ($n = 3$). (J) Levels of CDK6 and FN1 mRNA in the novel TTTY15 KO models: TKO2 and TKO8. $^{*}p < 0.05$ and $^{**}p < 0.01$, ANOVA ($n = 3$). (K) Levels of CDK6 and FN1 mRNA after transfection with the representative microRNA mimics of let-7a and let-7f. $^{*}p < 0.05$ and $^{**}p < 0.01$, ANOVA ($n = 3$). Levels of CDK6 and FN1 protein after (L) siRNA transfection and (M) TTTY15 KO, as well as (N) after transfection with the TTTY15 overexpression plasmid and TTTY15 mutant overexpression plasmid. (O) GSEA of all the let-7 target genes predicted by Miranda in TTTY15 knockout DU145 cell lines and control. Both enrichment score (–0.5362785 in TKO2 vs control,–0.5207912 in TKO8 vs control) results indicated that gene affected by let-7 miRNA family was found to be negatively enriched with the knockout of the TTTY15. ANOVA = analysis of variance; GSEA = gene set enrichment analysis; ISH = in situ hybridisation; KO = knockout; SD = standard deviation; TCGA = The Cancer Genome Atlas.

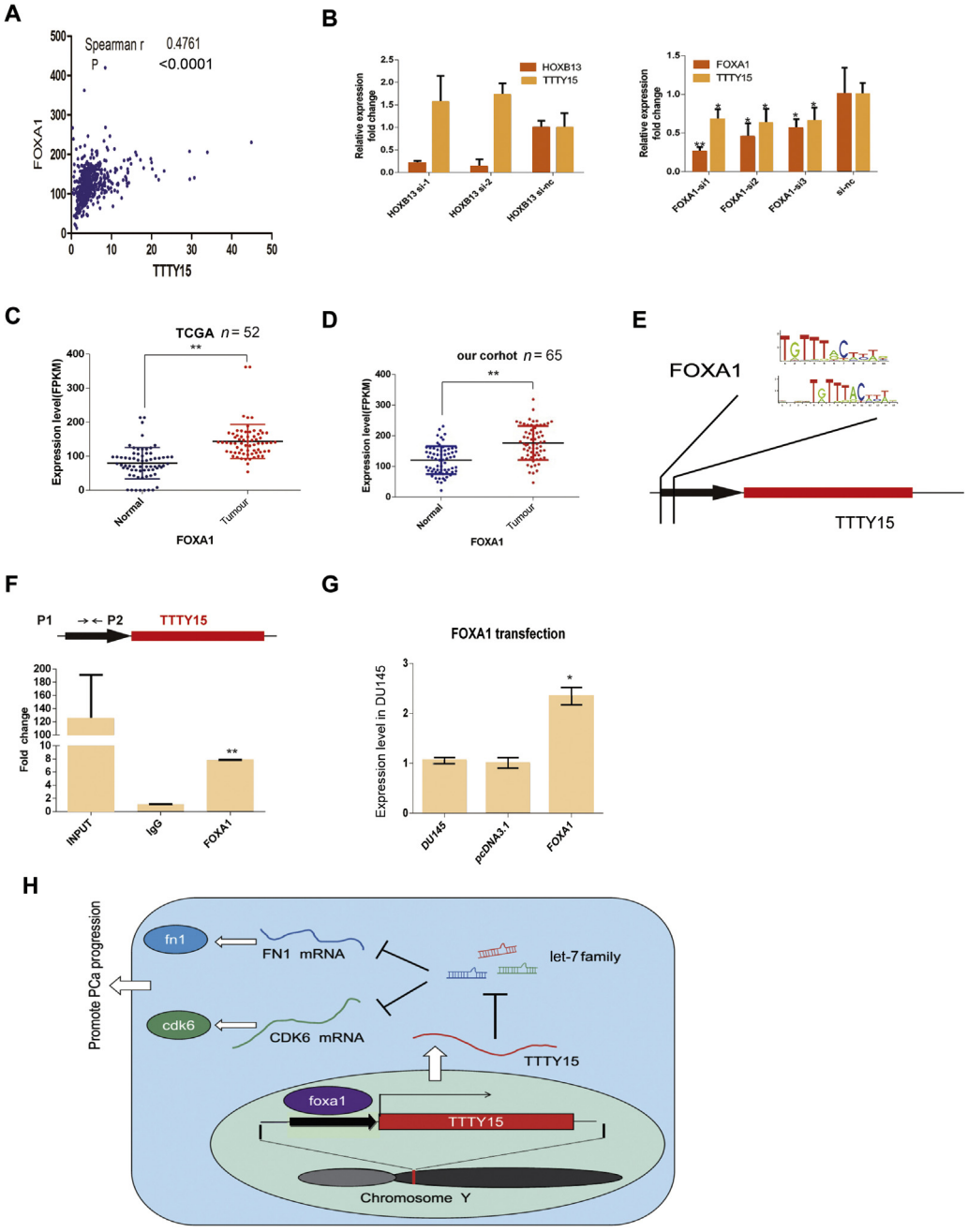

Fig. 6 – FOXA1 is an upstream transcription factor of TTTY15 in PCa cells. (A) The relationship between TTTY15 and FOXA1 expression levels. The data were mined from TCGA ($n = 551$). (B) Knockdown of FOXA1 decreased TTTY15 expression. RNA levels were analysed by qRT-PCR. Beta-actin was used as the reference. The data are presented as the mean ± SD. $^{*}p < 0.05$ and $^{**}p < 0.01$, ANOVA ($n = 3$). (C and D) FOXA1 levels were evaluated in prostate cancer samples from both our cohort (65 pairs) and TCGA database (52 pairs). $^{*}p < 0.05$ and $^{**}p < 0.01$, Wilcoxon matched-pair signed-rank test. (E) Putative binding sites for FOXA1 in the TTTY15 promoter region predicted by JASPAR. (F) ChIP-PCR validation of the binding sites. The data are presented as the mean ± SD of three independent experiments. $^{*}p < 0.05$ and $^{**}p < 0.01$, ANOVA. (G) TTTY15 levels after FOXA1 overexpression. RNA levels were assessed using qRT-PCR. Beta-actin was used as the reference. The data are presented as the mean ± SD. $^{*}p < 0.05$ and $^{**}p < 0.01$, ANOVA ($n = 3$). (H) A schematic representation of the regulatory network. Expression of the lncRNA TTTY15 located on the Y chromosome is upregulated by increased FOXA1 levels and then serves as a ceRNA by binding to microRNAs of the let-7 family. Sequestration of let-7 family members potentially upregulates the expression of oncogenes, such as CDK6 and FN1, which might support prostate cancer progression. ANOVA = analysis of variance; ceRNA = competing endogenous RNA; lncRNA = long noncoding RNA; PCa = prostate cancer; PCR = polymerase chain reaction; qRT-PCR = quantitative reverse transcription polymerase chain reaction; SD = standard deviation; TCGA = The Cancer Genome Atlas.

5. Conclusions

In summary, we found that the Y chromosome lncRNA TTTY15 was upregulated in most PCa samples. TTTY15 promoted PCa progression by acting as a ceRNA to sponge let-7, and tumour growth arrest was revealed after TTTY15 KO using our CRISPR/Cas9 strategies. As a monoallele on the Y chromosome, this gene has a unique advantage for gene

editing therapy, and thus, TTTY15 may have therapeutic implications for some PCa patients.

***Author contributions*:** Yinghao Sun had full access to all the data in the study and takes responsibility for the integrity of the data and the accuracy of the data analysis.

Study concept and design: Sun, Jiang, Xiao, Yao.
Acquisition of data: Xiao, Yao, Jiang, Kong.
Analysis and interpretation of data: Xiao, Yao, Kong, Jiang, Y. Wang.
Drafting of the manuscript: Jiang, Xiao.
Critical revision of the manuscript for important intellectual content: Xiao, Jiang, J. Li.
Statistical analysis: Xiao, Yao, Kong.
Obtaining funding: Sun, Jiang, Zhang.
Administrative, technical, or material support: Shi, Ye, Chen, L. Li, Zeng, L. Wang, Zhou, Y. Wang, Xu.
Supervision: Sun.
Other: None.

Financial disclosures: Yinghao Sun certifies that all conflicts of interest, including specific financial interests and relationships and affiliations relevant to the subject matter or materials discussed in the manuscript (eg, employment/affiliation, grants or funding, consultancies, honoraria, stock ownership or options, expert testimony, royalties, or patents filed, received, or pending), are the following: None.

Funding/Support and role of the sponsor: This study was supported by the National Natural Science Foundation of China (81430058, Yinghao Sun), Shanghai Science and Technology Commission (16YF1414800, Junfeng Jiang; 18YF1422600, Wei Zhang), and China Postdoctoral Science Foundation (2016M602989, Junfeng Jiang).

Appendix A. Supplementary data

Supplementary data associated with this article can be found, in the online version, at https://doi.org/10.1016/j.eururo.2018.11.012.

References

[1] Torre LA, Bray F, Siegel RL, Ferlay J, Lortet-Tieulent J, Jemal A. Global cancer statistics, 2012. CA Cancer J Clin 2015;65:87–108.
[2] Siegel RL, Miller KD, Jemal A. Cancer statistics, 2018. CA Cancer J Clin 2018;68:7–30.
[3] Chen W, Zheng R, Baade PD, et al. Cancer statistics in China, 2015. CA Cancer J Clin 2016;66:115–32.
[4] Ren S, Peng Z, Mao JH, et al. RNA-seq analysis of prostate cancer in the Chinese population identifies recurrent gene fusions, cancer-associated long noncoding RNAs and aberrant alternative splicings. Cell Res 2012;22:806–21.
[5] Labbe DP, Sweeney CJ, Brown M, et al. TOP2A and EZH2 provide early detection of an aggressive prostate cancer subgroup. Clin Cancer Res 2017;23:7072–83.
[6] Liang Y, Ahmed M, Guo H, et al. LSD1-mediated epigenetic reprogramming drives CENPE expression and prostate cancer progression. Cancer Res 2017;77:5479–90.
[7] Zhang C, Wang L, Wu D, et al. Definition of a FoxA1 Cistrome that is crucial for G1 to S-phase cell-cycle transit in castration-resistant prostate cancer. Cancer Res 2011;71:6738–48.
[8] Thomsen MK, Ambroisine L, Wynn S, et al. SOX9 elevation in the prostate promotes proliferation and cooperates with PTEN loss to drive tumor formation. Cancer Res 2010;70:979–87.
[9] Blattner M, Liu D, Robinson BD, et al. SPOP mutation drives prostate tumorigenesis in vivo through coordinate regulation of PI3K/mTOR and AR signaling. Cancer Cell 2017;31:436–51.
[10] Wu JB, Yin L, Shi C, et al. MAOA-dependent activation of Shh-IL6-RANKL signaling network promotes prostate cancer metastasis by engaging tumor-stromal cell interactions. Cancer Cell 2017;31:368–82.
[11] Liu C, Kelnar K, Liu B, et al. The microRNA miR-34a inhibits prostate cancer stem cells and metastasis by directly repressing CD44. Nat Med 2011;17:211–5.
[12] Yao L, Ren S, Zhang M, et al. Identification of specific DNA methylation sites on the Y-chromosome as biomarker in prostate cancer. Oncotarget 2015;6:40611–21.
[13] Zhu Y, Ren S, Jing T, et al. Clinical utility of a novel urine-based gene fusion TTTY15-USP9Y in predicting prostate biopsy outcome. Urol Oncol 2015;33, 384.e9–e20.
[14] Takahashi S, Alcaraz A, Brown JA, et al. Aneusomies of chromosomes 8 and Y detected by fluorescence in situ hybridization are prognostic markers for pathological stage C (pt3N0M0) prostate carcinoma. Clin Cancer Res 1996;2:137–45.
[15] Lindstrom S, Adami HO, Adolfsson J, Wiklund F. Y chromosome haplotypes and prostate cancer in Sweden. Clin Cancer Res 2008;14:6712–6.
[16] Wright DJ, Day FR, Kerrison ND, et al. Genetic variants associated with mosaic Y chromosome loss highlight cell cycle genes and overlap with cancer susceptibility. Nat Genet 2017;49:674–9.
[17] Forsberg LA, Rasi C, Malmqvist N, et al. Mosaic loss of chromosome Y in peripheral blood is associated with shorter survival and higher risk of cancer. Nat Genet 2014;46:624–8.
[18] Evans JR, Feng FY, Chinnaiyan AM. The bright side of dark matter: lncRNAs in cancer. J Clin Invest 2016;126:2775–82.
[19] Schmitt AM, Chang HY. Long noncoding RNAs in cancer pathways. Cancer Cell 2016;29:452–63.
[20] Prensner JR, Iyer MK, Sahu A, et al. The long noncoding RNA SChLAP1 promotes aggressive prostate cancer and antagonizes the SWI/SNF complex. Nat Genet 2013;45:1392–8.
[21] Zhang A, Zhao JC, Kim J, et al. LncRNA HOTAIR enhances the androgen-receptor-mediated transcriptional program and drives castration-resistant prostate cancer. Cell Rep 2015;13:209–21.
[22] Salameh A, Lee AK, Cardo-Vila M, et al. PRUNE2 is a human prostate cancer suppressor regulated by the intronic long noncoding RNA PCA3. Proc Natl Acad Sci USA 2015;112:8403–8.
[23] Prensner JR, Chen W, Iyer MK, et al. PCAT-1, a long noncoding RNA, regulates BRCA2 and controls homologous recombination in cancer. Cancer Res 2014;74:1651–60.
[24] Chakravarty D, Sboner A, Nair SS, et al. The oestrogen receptor alpha-regulated lncRNA NEAT1 is a critical modulator of prostate cancer. Nat Commun 2014;5:5383.
[25] Takayama K, Horie-Inoue K, Katayama S, , et al. Androgen-responsive long noncoding RNA. Androgen-responsive long noncoding RNA CTBP1-AS promotes prostate cancer. EMBO J 2013;32:1665–80.
[26] Ren S, Wei GH, Liu D, et al. Whole-genome and transcriptome sequencing of prostate cancer identify new genetic alterations driving disease progression. Eur Urol 2018;73:322–39.
[27] Wang Y, Xu Z, Jiang J, et al. Endogenous miRNA sponge lincRNA-RoR regulates Oct4, Nanog, and Sox2 in human embryonic stem cell self-renewal. Develop Cell 2013;25:69–80.
[28] Xu C, Zhang Y, Wang Q, et al. Long non-coding RNA GAS5 controls human embryonic stem cell self-renewal by maintaining NODAL signalling. Nat Commun 2016;7:13287.
[29] Wong N, Wang X. miRDB: an online resource for microRNA target prediction and functional annotations. Nucleic Acids Res 2015;43:D146–52.

[30] Betel D, Wilson M, Gabow A, Marks DS, Sander C. The microRNA.org resource: targets and expression. Nucleic Acids Res 2008;36:D149–53.
[31] Cannon-Albright LA, Farnham JM, Bailey M, et al. Identification of specific Y chromosomes associated with increased prostate cancer risk. Prostate 2014;74:991–8.
[32] Brothman AR, Maxwell TM, Cui J, Deubler DA, Zhu XL. Chromosomal clues to the development of prostate tumors. Prostate 1999;38:303–12.
[33] Jordan JJ, Hanlon AL, Al-Saleem TI, Greenberg RE, Tricoli JV. Loss of the short arm of the Y chromosome in human prostate carcinoma. Cancer Genet Cytogenet 2001;124:122–6.
[34] Khosravi P, Gazestani VH, Asgari Y, Law B, Sadeghi M, Goliaei B. Network-based approach reveals Y chromosome influences prostate cancer susceptibility. Comput Biol Med 2014;54:24–31.
[35] Wang Z, Parikh H, Jia J, et al. Y chromosome haplogroups and prostate cancer in populations of European and Ashkenazi Jewish ancestry. Hum Genet 2012;131:1173–85.
[36] Guo H, Ahmed M, Zhang F, et al. Modulation of long noncoding RNAs by risk SNPs underlying genetic predispositions to prostate cancer. Nat Genet 2016;48:1142–50.
[37] Sanchez-Rivera FJ, Jacks T. Applications of the CRISPR-Cas9 system in cancer biology. Nat Rev Cancer 2015;15:387–95.
[38] Jin HJ, Zhao JC, Wu L, Kim J, Yu J. Cooperativity and equilibrium with FOXA1 define the androgen receptor transcriptional program. Nat Commun 2014;5:3972.
[39] Jin HJ, Zhao JC, Ogden I, Bergan RC, Yu J. Androgen receptor-independent function of FoxA1 in prostate cancer metastasis. Cancer Res 2013;73:3725–36.
[40] Sunkel B, Wu D, Chen Z, et al. Integrative analysis identifies targetable CREB1/FoxA1 transcriptional co-regulation as a predictor of prostate cancer recurrence. Nucleic Acids Res 2016;44:4105–22.
[41] Jackstadt R, Roh S, Neumann J, et al. AP4 is a mediator of epithelial-mesenchymal transition and metastasis in colorectal cancer. J Exp Med 2013;210:1331–50.
[42] Gardi NL, Deshpande TU, Kamble SC, Budhe SR, Bapat SA. Discrete molecular classes of ovarian cancer suggestive of unique mechanisms of transformation and metastases. Clin Cancer Res 2014;20:87–99.
[43] Wang H, Nicolay BN, Chick JM, et al. The metabolic function of cyclin D3-CDK6 kinase in cancer cell survival. Nature 2017;546:426–30.